Data Mine

The MAGIC Experiment: A Combined Seismic and Magnetotelluric Deployment to Investigate the Structure, Dynamics, and Evolution of the Central Appalachians

Maureen D. Long*[1], Margaret H. Benoit[2], Rob L. Evans[3], John C. Aragon[1,4], and James Elsenbeck[3,5]

Abstract

The eastern margin of North America has undergone multiple episodes of orogenesis and rifting, yielding the surface geology and topography visible today. It is poorly known how the crust and mantle lithosphere have responded to these tectonic forces, and how geologic units preserved at the surface related to deeper structures. The eastern North American margin has undergone significant postrift evolution since the breakup of Pangea, as evidenced by the presence of young (Eocene) volcanic rocks in western Virginia and eastern West Virginia and by the apparently recent rejuvenation of Appalachian topography. The drivers of this postrift evolution, and the precise mechanisms through which relatively recent processes have modified the structure of the margin, remain poorly understood. The Mid-Atlantic Geophysical Integrative Collaboration (MAGIC) experiment, part of the EarthScope USArray Flexible Array, consisted of collocated, dense, linear arrays of broadband seismic and magnetotelluric (MT) stations (25–28 instruments of each type) across the central Appalachian Mountains, through the U.S. states of Virginia, West Virginia, and Ohio. The goals of the MAGIC deployment were to characterize the seismic and electrical conductivity structure of the crust and upper mantle beneath the central Appalachians using natural-source seismic and MT imaging methods. The MAGIC stations operated between 2013 and 2016, and the data are publicly available via the Incorporated Research Institutions for Seismology Data Management Center.

Cite this article as Long, M. D., M. H. Benoit, R. L. Evans, J. C. Aragon, and J. Elsenbeck (2020). The MAGIC Experiment: A Combined Seismic and Magnetotelluric Deployment to Investigate the Structure, Dynamics, and Evolution of the Central Appalachians, *Seismol. Res. Lett.* **XX**, 1–16, doi: 10.1785/0220200150.

Introduction

The eastern North American margin (ENAM), today a passive continental margin, has been modified by multiple episodes of orogenesis and rifting through two complete cycles of supercontinent assembly and breakup over the past billion years of Earth history. Major tectonic events that have affected the margin include the Grenville orogeny, associated with the formation of the Rodinia supercontinent (e.g., Rivers, 1997; McLelland *et al.*, 2010); the subsequent breakup of Rodinia (e.g., Li *et al.*, 2008); the various phases of the Appalachian orogeny (e.g., Hatcher, 2010; Hibbard *et al.*, 2010), which were associated with the accretion of multiple terranes onto the edge of Laurentia and which culminated in the formation of Pangea; and the breakup of Pangea during the Mesozoic (e.g., Frizon de Lamotte *et al.*, 2015). In addition to this established tectonic history, there are hints that the passive margin has undergone substantial postrift evolution since supercontinental breakup. For example, there is a temporally extensive history of postrift

1. Department of Geology and Geophysics, Yale University, New Haven, Connecticut, U.S.A.; 2. National Science Foundation, Alexandria, Virginia, U.S.A.; 3. Department of Geology and Geophysics, Woods Hole Oceanographic Institution, Woods Hole, Massachusetts, U.S.A.; 4. Now at Earthquake Science Center, U.S. Geological Survey, Menlo Park, California, U.S.A.; 5. Now at Lincoln Laboratories, Massachusetts Institute of Technology, Lexington, Massachusetts, U.S.A.

*Corresponding author: maureen.long@yale.edu

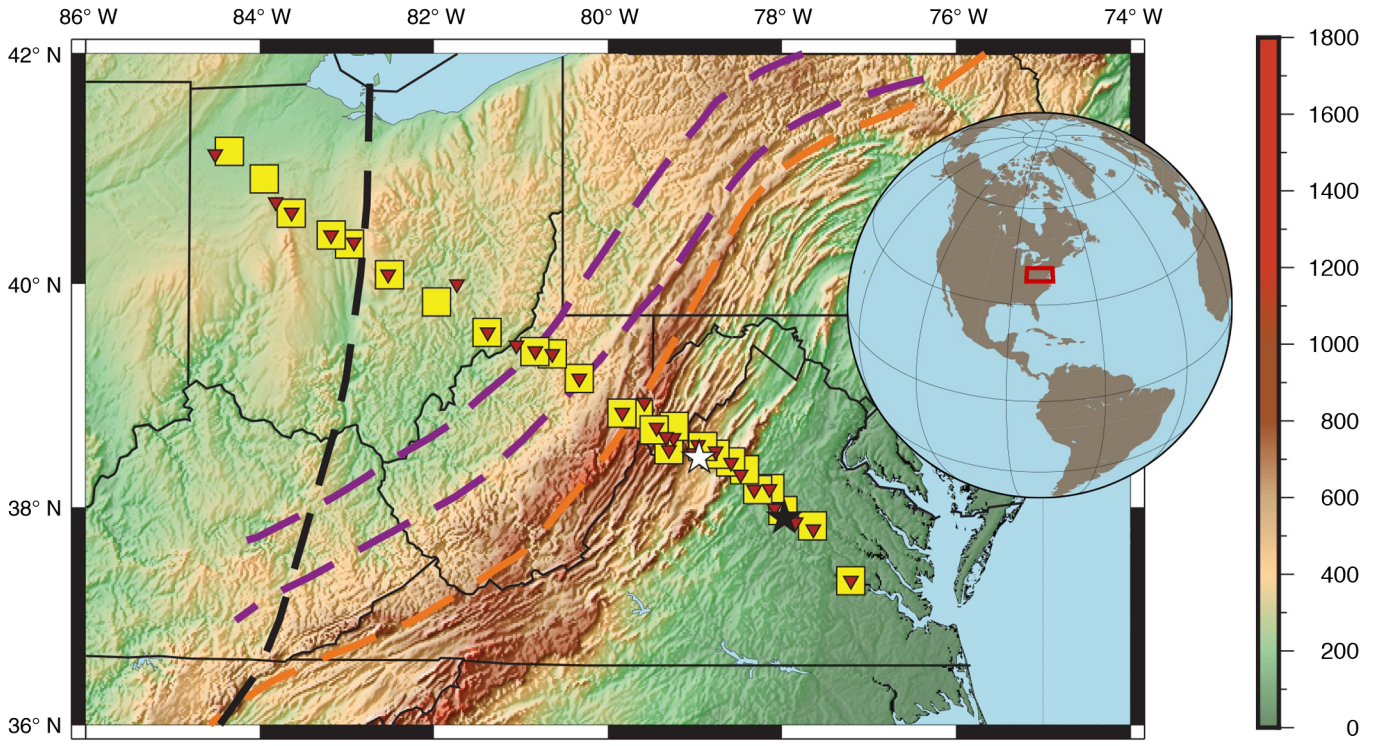

Figure 1. Map of Mid-Atlantic Geophysical Integrative Collaboration (MAGIC) seismic and magnetotelluric (MT) station locations. Inset map shows geographic location. Locations for seismic stations are shown with red triangles, and MT stations are shown with yellow squares. Background colors indicate topography (m), as shown by color bar at right. Thin black lines indicate state boundaries. Dashed lines show major tectonic features, including the putative Grenville Front (GF; black), as in Stein *et al.* (2018), boundaries of the Rome trough (RT; magenta), and the Appalachian Front (AF; orange) from Whitmeyer and Karlstrom (2007). Black star indicates the epicenter of the 2011 Mineral, Virginia, earthquake. White star indicates the location of Mole Hill, a topographically prominent volcanic neck of the Eocene (Mazza *et al.*, 2014). The color version of this figure is available only in the electronic edition.

volcanism along the margin (e.g., Mazza *et al.*, 2017), including a localized occurrence of magmatic activity during the Eocene in what is now western Virginia and eastern West Virginia (e.g., Mazza *et al.*, 2014). Furthermore, there is evidence from geomorphologic investigations that Appalachian topography has undergone relatively recent rejuvenation (e.g., Miller *et al.*, 2013). This may be due to flow in the deep mantle (e.g., Moucha *et al.*, 2008; Spasojevic *et al.*, 2008) or to temporal changes in the density structure of the crust (e.g., Fischer, 2002); alternatively, landscape transience may be due solely to surface processes. Finally, like many passive continental margins, ENAM plays host to significant seismicity, as evidenced by the 2011 magnitude 5.8 Mineral, Virginia, earthquake (e.g., Wolin *et al.*, 2012; McNamara *et al.*, 2014), which occurred in the central Virginia seismic zone (CVSZ).

With the advent of new geophysical data sets in eastern North America, such as the EarthScope USArray and the GeoPRISMS ENAM Community Seismic Experiment (Lynner *et al.*, 2020), we are in a position to gain new insights into the structure and dynamics of this passive margin. In this article, we describe the Mid-Atlantic Geophysical Integrative Collaboration (MAGIC) experiment, a combined seismic and magnetotelluric (MT) deployment across the central Appalachian Mountains that was part of the USArray Flexible Array. This project is aimed at studying the detailed structure of the crust, lithospheric mantle, asthenosphere, and mantle transition zone across this portion of ENAM. Our choice of target region in the central Appalachians (Fig. 1) affords us the opportunity to probe structure across Virginia, West Virginia, and Ohio, from the Coastal Plain in the east, across the present-day Appalachian Mountains, and extending west across the Grenville Front. The Grenville Front has typically been thought to represent the westward extent of deformation during Grenville orogenesis (e.g., Whitmeyer and Karlstrom, 2007), although recent work has proposed that this feature is instead associated with the Midcontinent Rift (e.g., Stein *et al.*, 2018; Elling *et al.*, 2020). We are particularly interested in understanding how the various episodes of orogenesis and rifting, associated with two complete Wilson cycles of supercontinent assembly and breakup, have affected the structure of the crust and lithospheric mantle, and in characterizing to what extent deep structures correspond to geologic units at the surface. An example of a specific target is the nature of the putative Grenville Front at depth, as constraints on its geometry and extent in the midcrust may shed light on its origin.

Furthermore, we wish to understand the processes associated with postrift evolution of the margin, including those that caused the Eocene magmatic event and those that may be responsible for the recent rejuvenation of Appalachian topography. Finally, we are interested in understanding the potential links between the structure of the crust and mantle lithosphere and the seismically active CVSZ.

Motivated by these scientific questions, the MAGIC field experiment was carried out across the central Appalachians between 2013 and 2016. This deployment, funded by the EarthScope and GeoPRISMS programs of the National Science Foundation (NSF), was a collaborative effort among seismology principal investigators (PIs) Maureen Long (Yale University) and Margaret Benoit (then at the College of New Jersey) and MTs PI Rob Evans (Woods Hole Oceanographic Institution [WHOI]). We deployed a linear array of (mostly) collocated broadband seismometers and long-period MT instruments across the U.S. states of Virginia, West Virginia, and Ohio (Fig. 1). Seismic data were collected starting in October 2013 and ending in October 2016. We deployed 28 broadband seismic sensors, with continuous data recording, and relied on natural (passive) earthquake sources. MT data were collected between October 2015 and May 2016, with each of the 25 MT sites being occupied for ~3 weeks; as with the seismic data, the MT experiment relied on natural sources. The MAGIC array crossed a number of geologic terranes and physiographic provinces, extending past the Grenville Front at its western end, and also intersected the CVSZ near its eastern end, passing close to the epicenter of the 2011 Mineral, Virginia, earthquake (Fig. 1). Our array also sampled the region affected by anomalous volcanic activity during the Eocene, with several stations deployed within a few kilometers of Eocene volcanic outcrops.

Instrument Deployment and Details

A map of all seismic and MT stations operated as part of the MAGIC experiment is shown in Figure 1. The MAGIC seismic array extended from Charles City, Virginia, to Paulding, Ohio, for an array aperture of ~770 km. A total of 29 sites were eventually occupied, with a maximum of 28 stations deployed at any given time (one station [TRTF] was relocated to a nearby site [MOLE] in summer 2015). The nominal station spacing was therefore just under 30 km, although we designed the array such that the station spacing was denser (~15 km) in the central portion (in the region with high topography and anomalous young volcanism) and less dense in the western portion (Fig. 1). We collected between 12 and 36 months of continuous data at each station. Deployment of the seismic instruments began in October 2013, when 13 stations were installed in Virginia and West Virginia. In this first phase of the seismic experiment, we deployed equipment owned by Yale University (Trillium 120PA broadband seismometers, paired with Taurus digitizer-datalogger, all manufactured by Nanometrics, Inc.). These instruments recorded data at 40 Hz sample rate on channels BHE, BHN, and BHZ. In October 2014, we took delivery of equipment from the Incorporated Research Institutions for Seismology (IRIS) Program for Array Seismic Studies of the Continental Lithosphere (PASSCAL) Instrument Center, which consisted of 28 Streckheisen STS-2 seismometers paired with Reftek RT-130 data loggers. During this phase of the experiment, we recorded data at 40 Hz sample rate on channels BHE, BHN, and BHZ, and also recorded at 1 Hz on channels LHE, LHN, and LHZ. We began to swap the PASSCAL equipment for the Yale-owned equipment in October 2014 and eventually converted all 13 of the original stations to PASSCAL equipment, in tandem with the deployment of newly installed stations. By the end of 2014, 23 stations were operating successfully. During the summer 2015 field season, we deployed additional four stations (all in Ohio) and relocated one (TRTF, in western Virginia). The final station was installed in October 2015, and the array was demobilized in October 2016. Service visits were carried out at approximately six month intervals; during service runs, we carried out a checklist to assess station health, swapped the data cards (all data were recorded locally to compact flash cards), and fixed any problems. After demobilization in October 2016, the equipment was cleaned, packed, and shipped back to PASSCAL. Field photos from the seismic experiment are shown in Figure 2.

Sites for seismic stations were chosen by conducting an initial survey of nominal locations on Google Earth. When possible, we contacted local businesses or nonprofit entities via email to identify landowners who were willing to host stations; in other cases, we relied on word of mouth recommendations or knocking on doors. In many cases, we contacted local colleges and universities for help in identifying station hosts. Several of our stations were located either on college property, including Denison University, Muskingum University, and Virginia Commonwealth University (VCU), or property owned by college faculty or staff or their contacts, including Randolph–Macon College, James Madison University (JMU), and Ohio Northern University (ONU). In several cases, these contacts with local colleges and universities allowed us to demonstrate equipment and discuss the scientific goals of the experiment with students and/or faculty during station installation and/or servicing. All stations were located on private property, with two exceptions, one (in Kenton, Ohio) that was located on the grounds of a town-owned park and another (in Charles City, Virginia) that was located on property owned by a public university (VCU).

Our seismic station design (Fig. 2) included a large (roughly 55 gal) high-density polyethylene barrel that was buried in the ground and served as a vault. Each barrel included a watertight lid that was sealed with a metal ring, with the sensor cable run through polyvinyl chloride (PVC) pipe out of the lid. The vault was seated in concrete to achieve coupling with the native soil, and additional concrete was poured into the barrel to serve as a

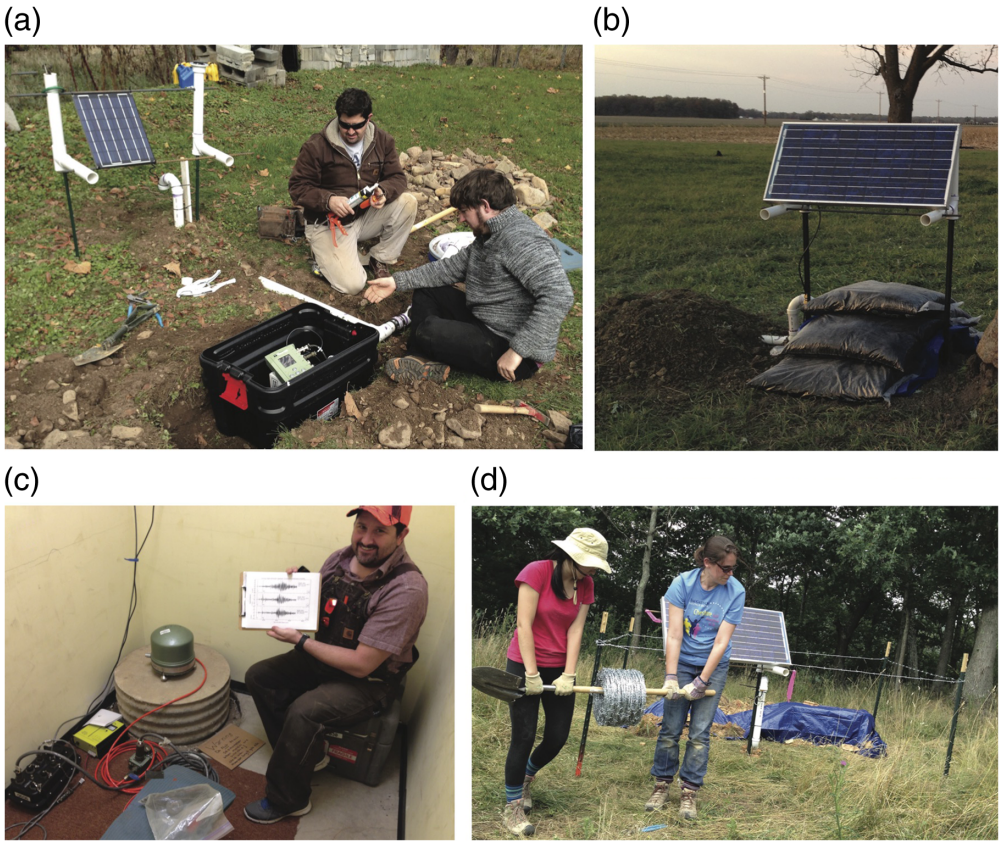

Figure 2. Field photos from the MAGIC seismic deployment. (a) Installation of station FOXP, located in Brandywine, West Virginia. Electronics were located in the partially buried ActionPacker in the foreground. Cables were threaded through white polyvinyl chloride (PVC) pipes arranged in a T shape that connects the vault (barrel with white lid, partially visible in background), the electronics box, and the solar panel mount (second panel has yet to be mounted). Field personnel are sealing cable entrance to electronics box with caulk. (b) A completed station (PAUL, located in Paulding, Ohio). The vault is located under the pile of dirt to the left (dirt pile provides thermal insulation). This station used a compact layout, in which the electronics box was located directly beneath the solar panels, under the bags of mulch, which are intended to keep the tarp in place in high winds. (c) Installation at station MUSK (located in New Concord, Ohio, at Muskingum University), which was deployed on a pier in the basement of the Boyd Science Center. (d) Construction of a barbed wire fence at station CAKE (Sugar Grove, West Virginia). The color version of this figure is available only in the electronic edition.

pad for the seismometer. We used an overturned plastic bucket as a sensor hut; after cutting a notch at the edge of the bucket to accommodate the sensor cable, the bucket was placed over the seismometer and two round pieces of rigid foam board insulation were placed on top of the bucket. This arrangement provided thermal insulation for the sensor, protecting it from diurnal temperature variations. Solar panels (two 36 W panels for the Nanometrics stations and one 65 W panel for the PASSCAL stations) were installed using a mount built of fence posts and PVC pipes; the Global Positioning System (GPS) clock antenna was mounted next to the solar panels. A series of 2″ PVC pipes (Fig. 2a) provided secure and waterproof housing for cables run from the sensor, the GPS antenna, and the solar panels to a partially buried Rubbermaid ActionPacker that functioned as a housing for the electronics. Power was provided by a battery (in most cases, a Sun Xtender 80 amp hour absorbent glass mat battery) charged by the solar panels. We did not typically fence around station installations, although two locations required barbed-wire fencing (Fig. 2d) to keep grazing cattle away from the equipment. Nearly all stations were located outdoors and used the standard station design; however, in one case (station MUSK), we installed a station indoors, on a seismic pier in the basement of the Boyd Science Center at Muskingum University (Fig. 2c). This station operated off A/C line power, with the GPS antenna mounted on the side of the building. We had no issues with security during the deployment, and no equipment was stolen or damaged by vandalism, although we had some issues with flooding of electronics boxes during year 1 of the deployment that was mitigated by repositioning them. Specifically, we reburied boxes that had flooded in a shallower position, so that they were less prone to flooding. Furthermore, after year 1 of the experiment, we added a small overturned plastic bin in each electronics box to serve as a "shelf" for the most vulnerable pieces of equipment (data loggers and solar regulator boxes), so they were kept off the floor of the ActionPacker and out of reach should flooding occur.

Wherever possible, MT stations were deployed at the same locations as seismic instruments. However, there are very different requirements for an ideal MT station compared to a seismic installation. MT acquisition is greatly affected by cultural noise from power lines, buried pipelines with cathodic protection, and other sources of electromagnetic noise related to infrastructure. We therefore typically try to site MT installations as far away (several kilometers) from these sources of noise as is reasonably possible. In some cases, this meant

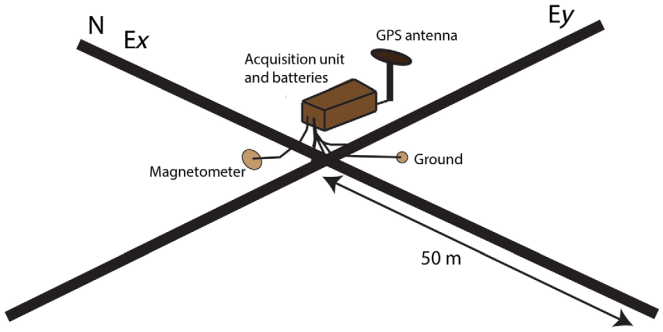

Figure 3. A schematic layout of an MT station. GPS, Global Positioning System. The color version of this figure is available only in the electronic edition.

finding different land owners for installation permission for MAGIC MT sites.

An MT installation is relatively straightforward and can be completed in 2–3 hr, depending on size of the field crew. Acquisition of MT data requires measuring naturally occurring electric and magnetic fields. To measure electric fields, an MT station (Fig. 3) will typically consist of two orthogonal electrode lines. Where possible, the electrode lines are oriented north–south and east–west and have a nominal length of 100 m, with 4×50 m lengths of insulated copper wire forming a cross shape on the ground. At its outer end, the length of wire is connected to an electrode that is buried in the ground. We used a combination of silver–silver chloride electrodes manufactured at WHOI and $Pb - PbCl_2$ gel-type electrodes made at Oregon State University (OSU). There are a number of approaches to burying electrodes to maintain a stable and damp environment, thus ensuring low impedance between the electrode and the ground. We adopted a method colloquially known as the "Russian Bucket" in which the electrode is placed in a small plastic bucket filled with a mix of bentonite clay (or clay rich soil) and saturated with a brine. The bucket with electrode is buried at a depth of ~70 cm–1 m, such that when the hole is infilled, the electrode is not affected by diurnal temperature variations. At the center of the cross, in which the four electrodes lines meet, they connect to a data acquisition unit. A fifth electrode is set up near the acquisition unit to provide a ground reference. Additional details on electrode chemistry and MT deployment strategies can be found in Ferguson (2012).

We used two systems for this survey: LEMI-417 owned by WHOI and Narod Geophysics Narod Intelligent Magnetotelluric Systems instruments made available by the National Geo-electromagnetic Facility at OSU. Each unit was connected to a three-component fluxgate magnetometer that records naturally occurring variations in magnetic field. Both recorded data at 1 Hz and provided MT responses from ~10 to around 20,000 s periods, depending on signal quality and noise levels. The time period of our survey (2015–2016) occurred in the middle of the sunspot cycle, with moderate levels of activity. Data acquisition units were housed in locked metal boxes for protection from theft and animals and deployed for around three weeks. Power was supplied by 12 V deep-cycle marine lead–acid batteries. During the deployment, we had one box that had been apparently attacked by bears, as the box holding the electronics was overturned and suffered some damage (there was no damage to the instrumentation, however). Interactions between bears and geophysical instrumentation have been previously documented in other settings (Tape *et al.*, 2019), particularly at remote locations.

Data Quality and Availability

Data and associated metadata from the MAGIC experiment are archived with the IRIS Data Management Center (DMC), are publicly available, and can be accessed with the full suite of DMC data-access tools. The seismic waveforms (network code 7A; see Data and Resources) were archived at the DMC beginning in 2014; although most data was embargoed for a period that extended until 2 yr after the end of the experiment (consistent with NSF and PASSCAL data-sharing policies), it was released to the public in late 2018. Data from one station (CABN, located in Riverton, West Virginia) was publicly available from the time the data were initially archived. The MT response functions (network code EM; see Data and Resources) are similarly archived at the IRIS DMC. We are currently working with the IRIS DMC to archive the MT time series; this will be completed once a new protocol for uploading MT time-series data is in place, as the DMC is currently in the process of migrating to a new format for such data.

We note that other broadband seismic or long-period MT instruments were deployed in our field area either before, during, or after our experiment, and data from these networks were also incorporated into several of the analyses described in the following. Other relevant networks include the U.S. National Seismic Network (network code US; see Data and Resources), the seismic USArray Transportable Array (network code TA; see Data and Resources), the seismic central and eastern United States Network (network code N4; see Data and Resources), and the MT USArray Transportable array (network code EM; see Data and Resources).

In general, the data quality from the MAGIC seismic array was high, although there were a few notable issues, particularly challenges with power failures during the first year of the deployment. Figure 4 shows a matrix of data availability and downtime for the seismic stations, highlighting data gaps of greater than 10,000 s. On average, the MAGIC seismic experiment had 86% data return, although the data return for the period between October 2014 and October 2016, during which the PASSCAL stations were deployed, was substantially higher (95%). Notably, a number of Nanometrics stations that were deployed in October 2013 had power failures at some point during the year; for several of these stations (BARB,

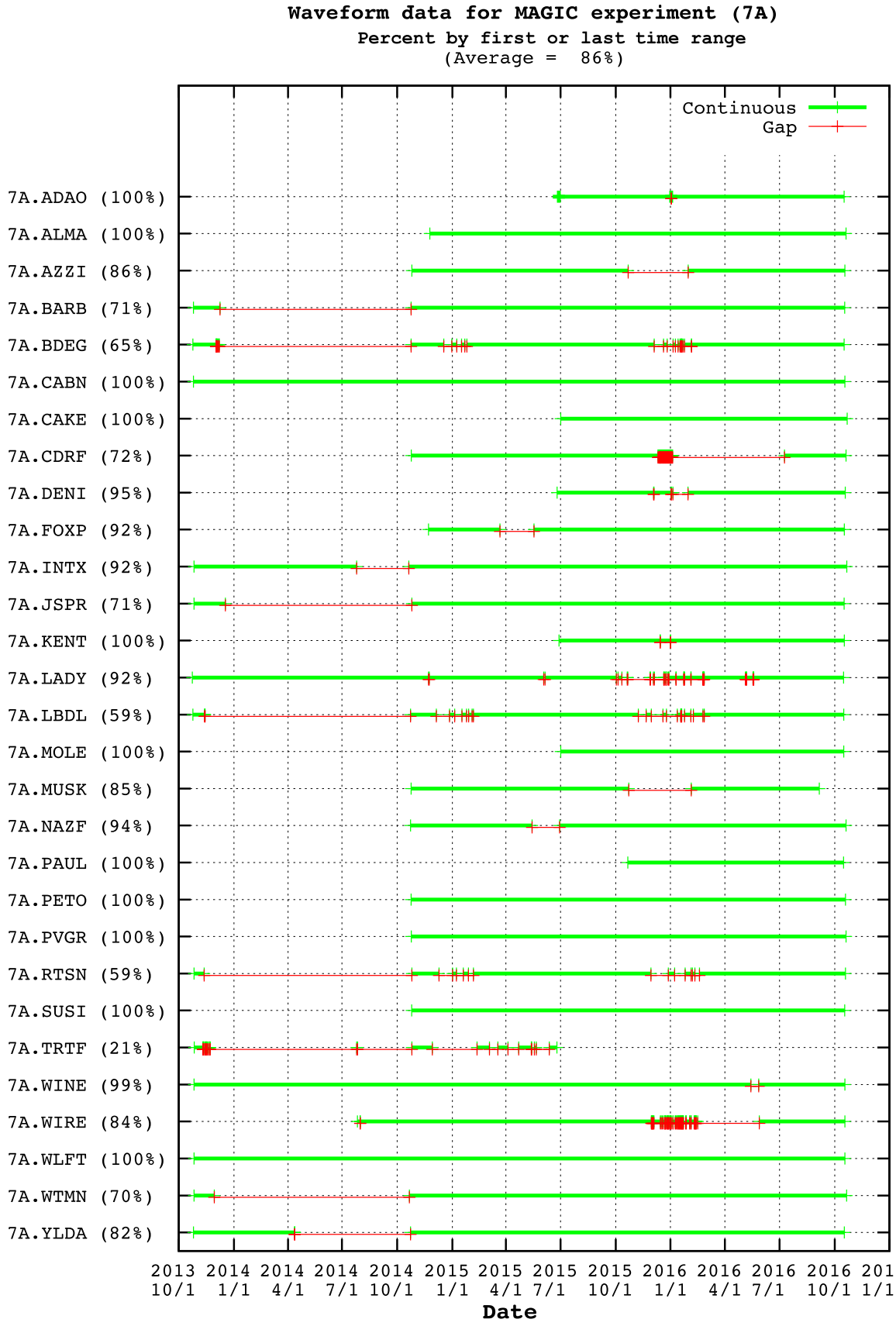

Figure 4. Matrix of data availability for the MAGIC seismic deployment. Individual stations are shown on the *y* axis, whereas the *x* axis indicates time (from October 2013 to October 2016). Periods of continuous data availability are shown with green lines, whereas gaps of greater than 10,000 s are shown with red lines. The color version of this figure is available only in the electronic edition.

BDEG, JSPR, LBDL, RTSN, TRTF, and WTMN), we only recorded a few months of data during the first year of the experiment. It was later determined that the suggested power settings (specifically, the low voltage disconnect and reconnect values) provided by the manufacturer for the deployment were incorrect, such that the instruments did not power back on after a loss of power. (This problem was corrected for subsequent deployments of the same equipment.) In the October 2014 to October 2016 period, data return was generally excellent, with just a few stations suffering from significant downtime (AZZI, CDRF, MUSK, and WIRE). We had one station (AZZI) that suffered from persistent problems with the seismometer coming out of level. The instrument was installed in October 2014 and came out of level in early January 2015; it was leveled during the May 2015 service run but came out of level again sometime between October 2015 and late January 2016 (the exact date is not known, as the data logger was not recording during this time). Because the seismometer feet were properly locked throughout this time, we speculate that the vault itself may have shifted, perhaps due to frost heaving, although there was no direct visual evidence of this at the station. The instrument was releveled for the last time in January 2016 and remained level for the rest of data collection.

We interrogated the noise profiles of our seismic stations by constructing power spectral density (PSD) plots using the MUSTANG tool (Casey *et al.*, 2018) provided by the IRIS DMC. Figure 5 shows a suite of probability density functions (PDFs) of PSDs for representative stations of the MAGIC seismic experiment and compares them to high- and low-noise models of Peterson (1993). These PDFs exhibit a typical shape, with a peak in the microseismic noise band (~5–10 s). For representative station CAKE (Fig. 5a–c), the vertical component shows lower noise levels than the horizontal components, as expected. The mode of the PDFs lies between the high- and low-noise models at all period ranges; for the vertical component (BHZ; Fig. 5c), it is closer to the low-noise model, particularly at longer periods (greater than ~10 s). A comparison of PDFs for vertical components at four different stations (Fig. 5c–f) illustrates the variability among stations of the experiment. The mode of the PDF lies between the high- and low-noise models for all stations at all period ranges. In the microseismic noise band, it lies roughly halfway between the high- and low-noise models at all stations, whereas at long periods (longer than 10 s), it is much closer to the low-noise model, except at station MUSK (New Concord, Ohio). MUSK, which was located on a seismic pier in the basement of a building at Muskingum University, also had substantially higher noise levels at higher frequencies (periods between 0.1 and 1 s) than other stations, likely due to its location in a high-use building.

Given the generally high data quality and good data return for the MAGIC seismic experiment, the coverage and completeness of the seismic data set is more than sufficient for the analyses we have applied. In Figure 6a, we show a record section of data recorded across the MAGIC array for the September 2015 magnitude 8.3 Illapel, Chile, earthquake (e.g., Li *et al.*, 2016), a shallow thrust event that occurred at an epicentral distance of ~71° from the center of the array. Of 28 MAGIC seismic stations, 27 were operating at this time (station PAUL was not installed until October 2015). Figure 6a demonstrates clear arrivals of both body waves and surface waves across the array. We recorded a large number of high-quality teleseisms during the period of the experiment, providing ample sources for analyses that rely on teleseismic events. Figure 6b shows the locations of earthquakes of magnitude greater than 5.8, at epicentral distances of 40° and greater, that occurred within the time period of our experiment (October 2013–October 2016).

Much of the eastern United States, including the mid-Atlantic region, is problematic for MT acquisition because of the high population density that brings high levels of cultural electromagnetic noise related to infrastructure. Data quality for the MT stations was moderate to good, with somewhat noisy signal levels observed across the mountains. MT time-series data were processed and converted to response functions using the bounded influence code, BIRRP (Chave and Thomson, 2004). MT observations from adjacent sites and the INTERMAGNET observatory network were used as remote references. Some sites that had poor-quality responses on first processing were reprocessed using an algorithm designed for data with nonstationary noise issues (Neukirch and Garcia, 2014), which improved the quality of the response curves.

Derived MT responses generally span the period band from 10 to ~10, 000 s, with some variability in quality at either end of the period band. Phase-tensor ellipses (e.g., Caldwell *et al.*, 2004) are shown for the MAGIC MT data at periods of 1196 s in Figure 7. These ellipses provide a graphical means of demonstrating the dimensionality of the impedance tensor. Near circular ellipses, with low skew values, are indicative of 1D resistivity structure beneath a station. Because structure becomes more complex, the ellipticity increases. Figure 8 shows examples of response functions at four selected MAGIC MT stations (P004, P013, P020, and P025), plotted as apparent resistivity and phases for the off-diagonal (*xy* and *yx*) and diagonal (*xx* and *yy*) components of the impedance tensor.

Initial Observations, Results, and Future Directions

A suite of analysis tools and techniques have already been applied to the seismic and MT data collected during the MAGIC experiment, including inversion for 2D and 3D electrical conductivity models (Evans *et al.*, 2019), *SKS* splitting analysis (Aragon *et al.*, 2017), *Ps* receiver function (RF) analysis for characterizing crustal structure (Long *et al.*, 2019), *Sp* RF analysis for analyzing lithospheric structure (Evans *et al.*, 2019),

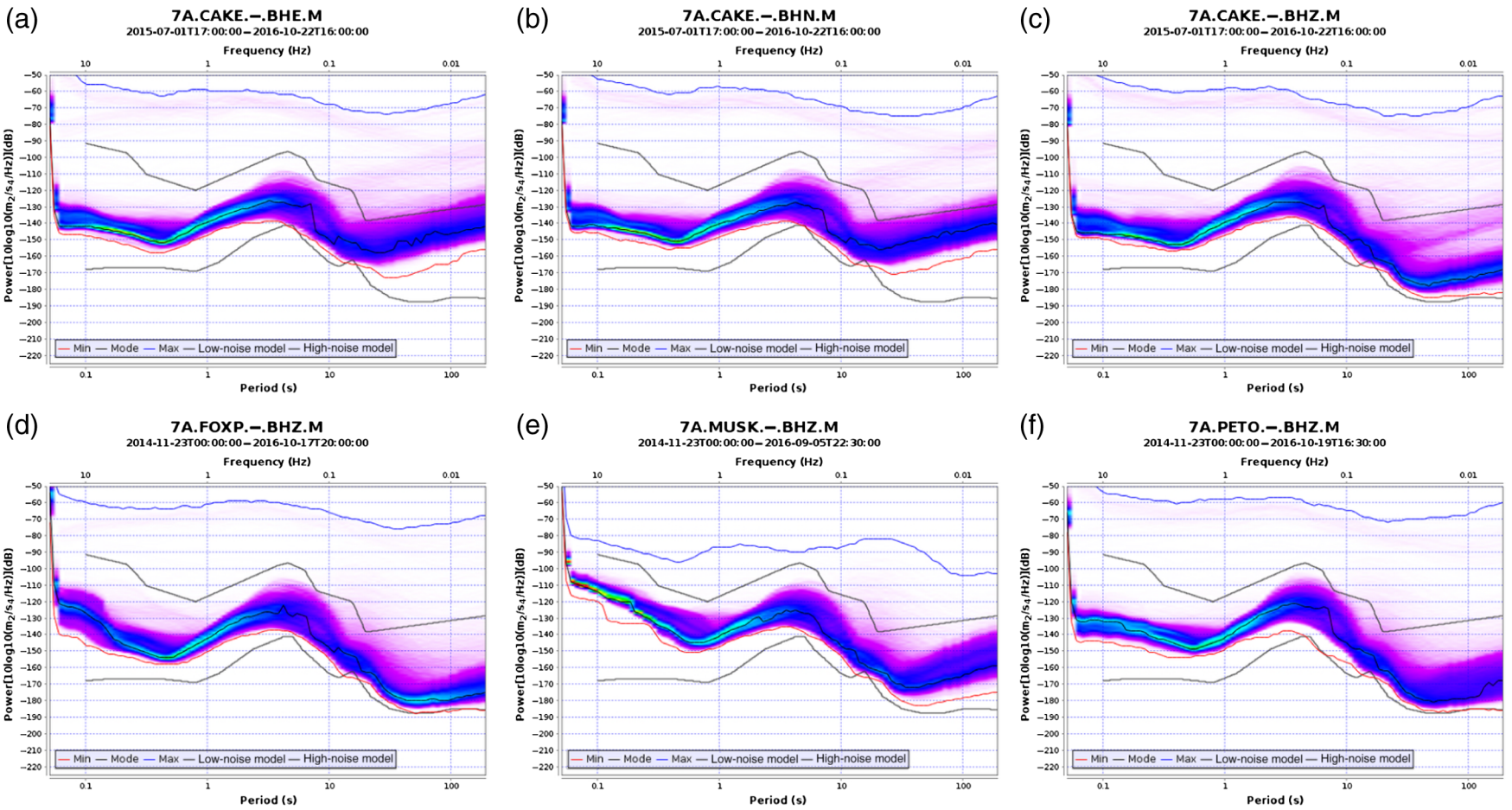

Figure 5. Examples of probability density functions (PDFs) of power spectral density (PSD) plots (power in decibels as a function of period in seconds), generated using the IRIS MUSTANG tool (Casey *et al.*, 2018), showing noise levels at MAGIC seismic stations. (a)–(c) PSDs for a representative station (CAKE, located in Sugar Grove, West Virginia) for channels (a) BHE, (b) BHN, and (c) BHZ. (d)–(f) PSDs for BHZ components for three additional stations for comparison, including one station (FOXP, located in Brandywine, West Virginia) sited within ~150 yards of a major road (U.S. Route 33), one station (MUSK, located in New Concord, Ohio) located on a seismic pier in the basement of a university building, and one station (PETO, located in Lost Creek, West Virginia), located in a particularly quiet area. On each plot, the color scale indicates the density, and the minimum, maximum, and mode of the data are shown as indicated in the legend. The high- and low-noise models of Peterson (1993) are also indicated. The color version of this figure is available only in the electronic edition.

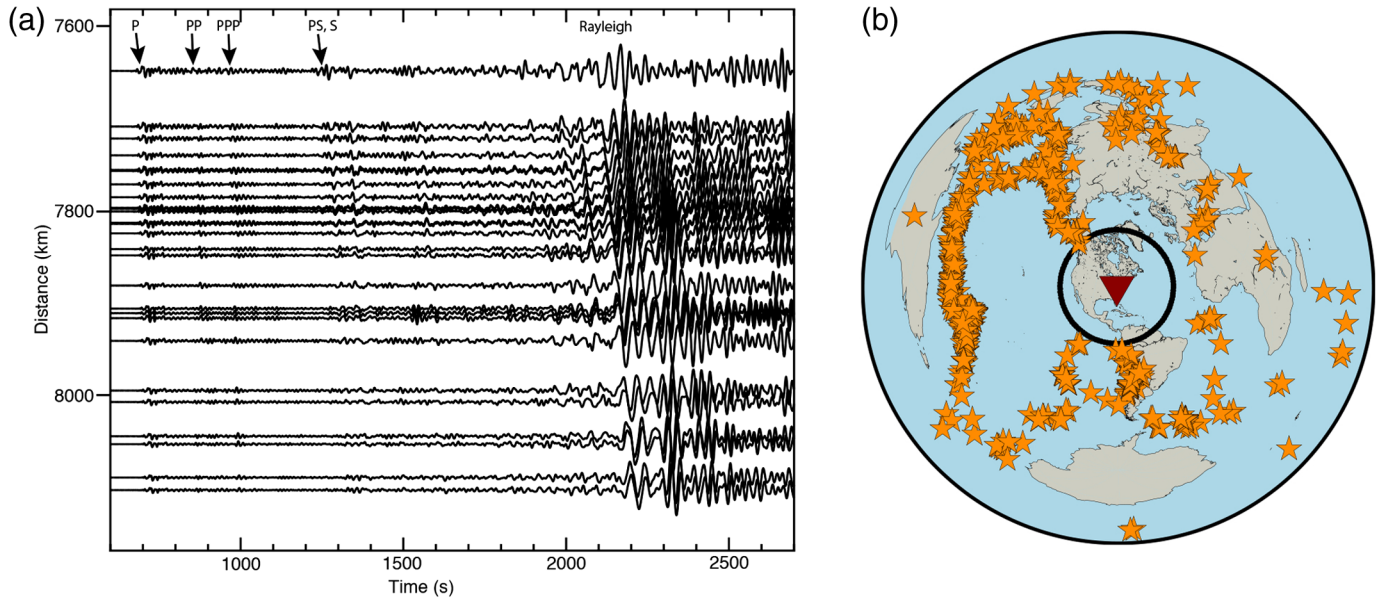

Figure 6. (a) Vertical-component record section showing recordings at MAGIC stations of the September 2015 magnitude 8.3 earthquake near Illapel, Chile. Major body- and surface-wave phases are labeled. (b) Map of teleseismic events (yellow stars) of magnitude 5.8 and greater at epicentral distances beyond 40° (black circle) during the time of the deployment (October 2013–October 2016). The center of the MAGIC array is marked with a red triangle. The color version of this figure is available only in the electronic edition.

estimation of body-wave attenuation structure (Byrnes *et al.*, 2019), and analysis of Love to Rayleigh surface-wave scattering (Servali *et al.*, 2020). Each of these published results is briefly described in the following. In addition to these studies, several analyses of MAGIC data are in progress within our research groups. These include applications of *SKS* splitting intensity tomography (Mondal and Long, 2019) to MAGIC data (Borden *et al.*, 2019), investigations of mantle transition zone structure beneath the MAGIC array using *Ps* RFs (Liu *et al.*, 2018), and joint analysis of RF data and gravity data to determine crustal structure and interrogate its possible links with the seismically active CVSZ (Long and Benoit, 2017). We also have efforts underway to analyze body-wave travel-time residuals, carry out anisotropy-aware finite-frequency body-wave tomography, apply full-wave ambient noise tomography to probe crustal structure, implement scattered-wave migration imaging, conduct anisotropy-aware *Ps* RF analysis, and jointly invert MT and surface-wave data to more fully characterize lithospheric structure. In addition to these data analysis projects, we are currently undertaking multidisciplinary studies to synthesize geophysical imaging results with complementary investigations of the central Appalachians (e.g., Mazza *et al.*, 2014; Wagner *et al.*, 2018), and with constraints from other components of the MAGIC collaborative project, which included geodynamical modeling (Liu and King, 2019) and geomorphology investigations (Miller *et al.*, 2015). Finally, we are aware of several published studies by other research groups that use MAGIC data (e.g., Biryol *et al.*, 2016; Lai *et al.*, 2019; Kintner *et al.*, 2020) and strongly encourage other researchers to make use of the data set.

Investigations into the anisotropic structure of the upper mantle using MAGIC data have included *SKS* splitting measurements (Aragon *et al.*, 2017) and analysis of Love- to Rayleigh-wave scattering (Servali *et al.*, 2020) using data from both MAGIC and the USArray Transportable Array. Aragon *et al.* (2017) found evidence for small-scale lateral variations in azimuthal anisotropy along the MAGIC line, with a sharp transition in shear-wave splitting behavior between stations located in the Appalachian Mountains (with generally orogen-parallel fast directions and ~1 s delay times) and stations located just to the east (with east–west fast directions and markedly smaller delay times). We carried out two-layer modeling of the observations, which supported the idea of distinct lithospheric and asthenospheric anisotropy regimes. Aragon *et al.* (2017) proposed a scenario in which *SKS* splitting beneath the Appalachians reflects lithospheric deformation associated with orogenesis, whereas just to the east, the anisotropic signature in the lithosphere was modified by rifting associated with the breakup of Pangea. Servali *et al.* (2020) identified evidence for the presence of scattered quasi-Love phases from teleseismic earthquakes on seismograms from stations throughout eastern North America, including MAGIC stations. They found that the scattering points associated with the quasi-Love phases preferentially sampled the central portion of ENAM, with most scattering points located just offshore. This was thought to reflect a local transition in anisotropy in the asthenospheric mantle, likely associated with complex and 3D mantle flow, as previously suggested based on *SKS* splitting data (Lynner and Bodmer, 2017).

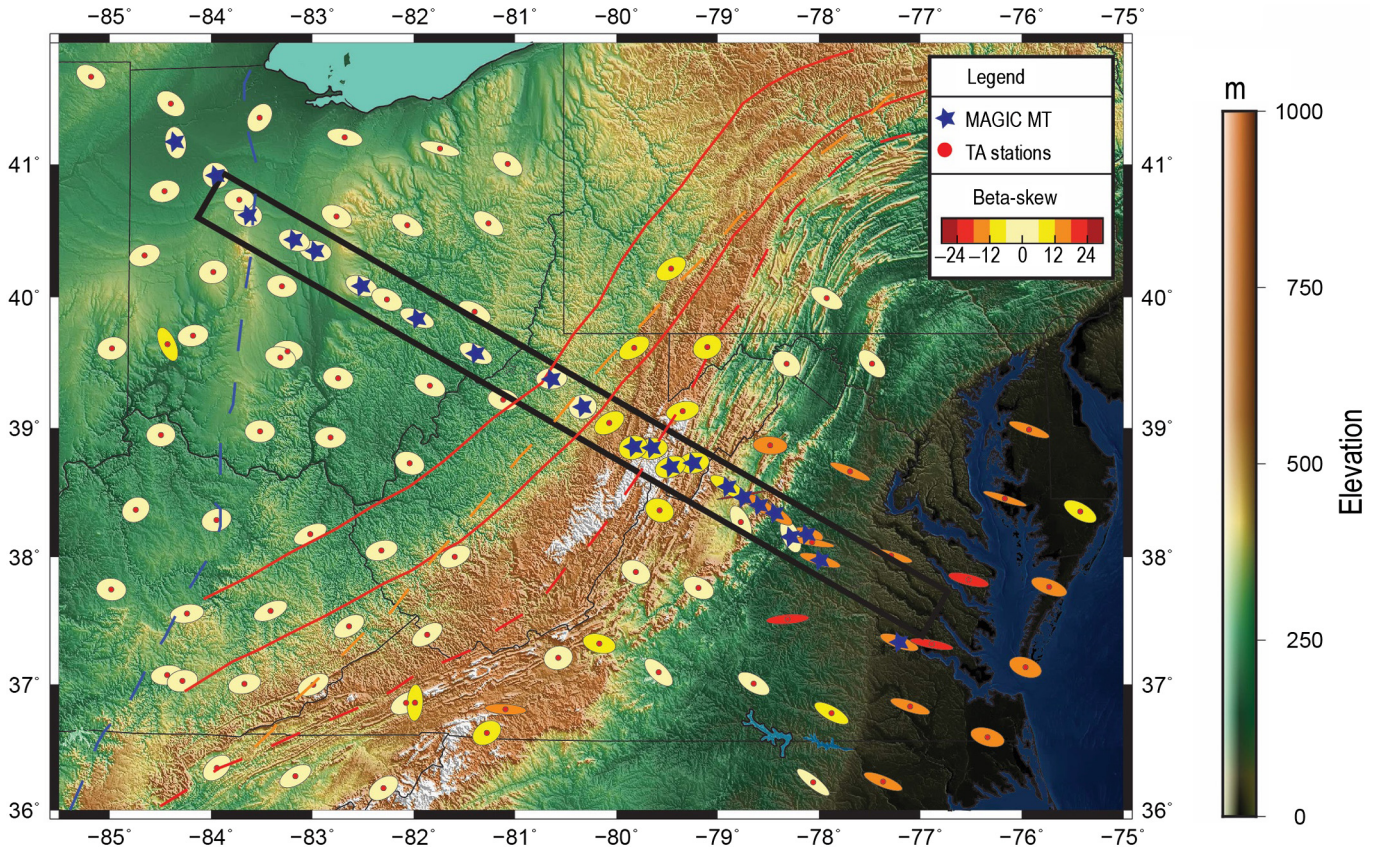

Figure 7. Map of phase tensor ellipses (skew) at MAGIC and Transportable Array MT stations, modified from Evans *et al.* (2019). The location of the primary MAGIC line lies within the black box. Phase-tensor ellipses of each MT station at a period of 1196 s (approximately sensing structure at mantle depths) are plotted and infilled by beta-skew values. There is a clear gradient in beta-skew and ellipticity, with values increasing toward the coastline. The blue line shows the approximate location of the Grenville Front, the red lines bracket the Rome trough, the dashed orange line is the New York–Alabama Lineament (Steltenpohl *et al.*, 2010), and the red dashed line marks the Appalachian Front. The color version of this figure is available only in the electronic edition.

Long *et al.* (2019) presented constraints on crustal structure beneath the MAGIC experiment based on *Ps* RF analysis. The dense station spacing of the array (~15 km in its densest portion) allowed us to obtain unaliased imaging of mid-to-lower crustal structure in most portions of the study region. Our RF images (Fig. 9) reveal evidence for significant variations in crustal thickness across the array, from ~32 km in the eastern portion to a maximum of ~58 km beneath central Ohio. Moho depths beneath the Appalachian Mountains are ~50–55 km, somewhat larger than would be expected given the relatively modest topography (Fig. 9) if simple Airy isostacy was assumed. We documented evidence for local crustal thinning beneath the Rome Trough (Fig. 9), a Cambrian rift structure associated with the breakup of Laurentia. In addition to this variability in crustal thickness, we identified a midcrustal negative velocity gradient in the western half of the array. This feature dips gently (apparent dip angle <10°) to the southeast and extends east from a location near the Grenville Front (Whitmeyer and Karlstrom, 2007), appearing to terminate near the Appalachian Mountains. Our preferred interpretation is that this feature corresponds to an anisotropic intracrustal shear zone associated with collisional deformation, most likely during Grenville orogenesis. The MAGIC seismic experiment has thus identified evidence of tectonic features in the midcrustal record, which has been preserved through the last billion years of Earth history. Furthermore, the similarity between the negative velocity gradient feature (Fig. 8) and midcrustal features that have been identified in other orogens, both ancient (Appalachians; Hopper *et al.*, 2017) and modern (Himalayas; Schulte-Pelkum *et al.*, 2005), suggests that similar styles of crustal deformation during continental collisional orogenesis have persisted over long periods of Earth history.

Data from the MAGIC experiment have yielded several lines of evidence for lithospheric loss beneath the central Appalachians, and this represents one of the major findings of the project to date. In two recently published companion articles, we presented measurements of body-wave attenuation across the MAGIC seismic array (Byrnes *et al.*, 2019) and a combined analysis of the MAGIC electrical conductivity model and *Sp* RF gathers (Evans *et al.*, 2019). Byrnes *et al.* (2019)

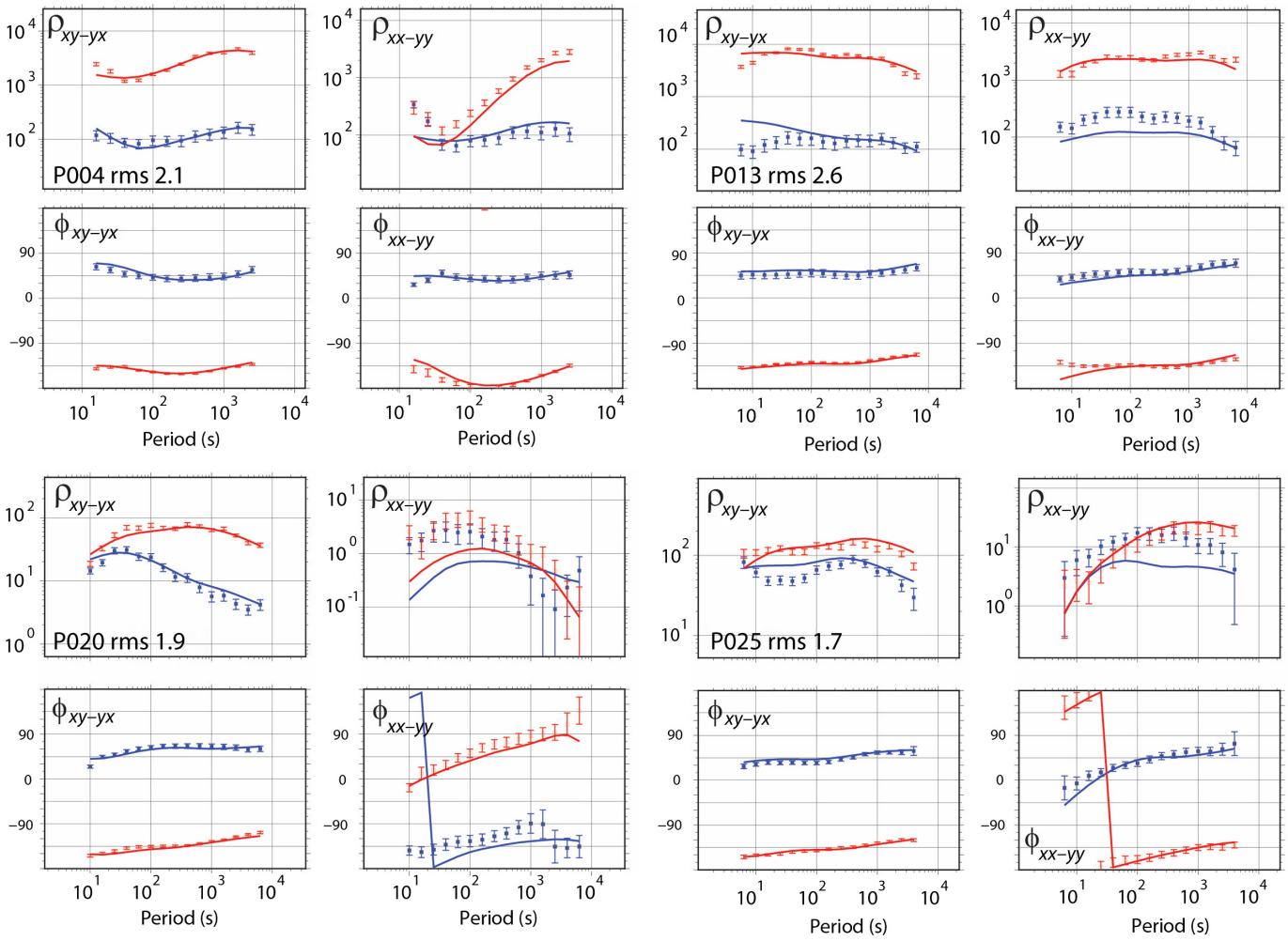

Figure 8. Example MT impedance tensors for four MAGIC stations, modified from Evans *et al.* (2019). These responses are plotted as apparent resistivity ρ ($\Omega \cdot$ m) and phase ϕ (°) for the off-diagonal (*xy*, red and *xy*, blue) and diagonal (*xx*, red and *yy*, blue) components of the impedance tensor. The smooth curves show the predicted responses for the preferred 3D electrical conductivity model presented in Evans *et al.* (2019). rms, root mean square. The color version of this figure is available only in the electronic edition.

measured lateral variations in the attenuation of teleseismic *P* waves and found a pronounced anomaly in attenuation parameter directly beneath the Appalachian Mountains, with strong attenuation directly beneath this region. This pattern is most easily explained by the presence of thin lithosphere beneath the mountains, with thicker lithosphere to the east and (especially) west, consistent with a past lithospheric loss event. Simple modeling carried out by Byrnes *et al.* (2019) suggests that partial melt in the asthenospheric mantle may be required to explain the inferred values of Q_p (quality factor). Evans *et al.* (2019) likewise found evidence for thin lithosphere directly beneath the Appalachians, based on complementary constraints from the MT and seismic components of the MAGIC experiment. The electrical conductivity model derived from MAGIC MT data (Fig. 10a) exhibits a strong low-resistivity anomaly, consistent with asthenospheric upper mantle (perhaps with a small amount of partial melt) that extends nearly to the base of the crust (depths of ~70–80 km) directly beneath the Appalachian Mountains. On either side of this anomaly, higher resistivity values are present, suggesting thicker lithosphere. Constraints on lithospheric architecture from *Sp* RF analysis, also reported in Evans *et al.* (2019), support this interpretation; we imaged a shallow, westward-dipping converter (feature labeled B in Fig. 10b), beneath the Appalachians that we infer represents the lithosphere–asthenosphere boundary. Taken together, the electrical conductivity model and *Sp* RF image (Fig. 10), along with the attenuation measurements of Byrnes *et al.* (2019), are strongly suggestive of thinned lithosphere beneath the central Appalachians, spatially coincident with the Eocene volcanics. We hypothesize that a lithospheric loss event during the Eocene is the most likely explanation for these observations; this scenario is consistent with suggestions made by Mazza *et al.* (2014) based on the geochemistry and petrology of Eocene basalts from our study area.

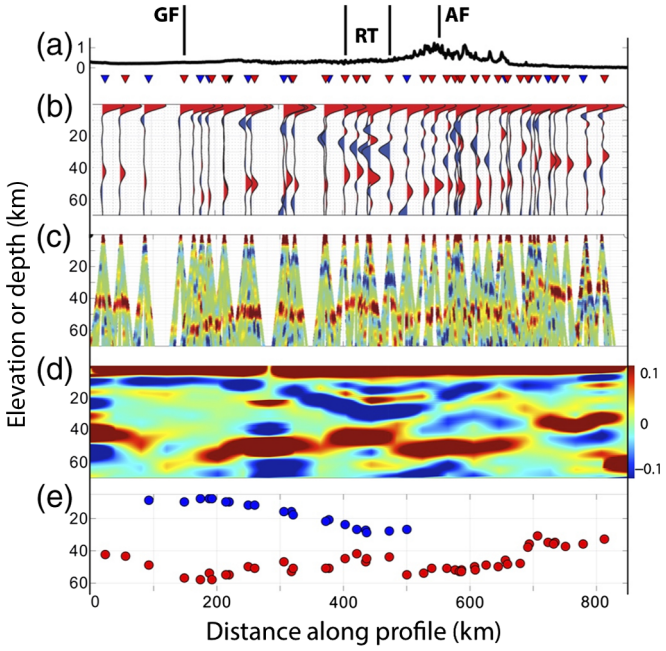

Figure 9. Images of the crust across the MAGIC array derived from *Ps* receiver function (RF) analysis, modified from Long *et al.* (2019). Profiles run from northwest (left) to southeast (right). (a) The profile, with triangles indicating station locations (red for MAGIC stations, blue for other stations) and vertical lines indicating major tectonic features, labeled as in Figure 1. (b) Single-station stacked radial RF traces, migrated to depth (*y* axis, in kilometers) and plotted at station location (distance along transect on *x* axis, in kilometers). Note vertical exaggeration of the image. Red pulses correspond to a positive velocity gradient with depth; blue pulses correspond to a negative velocity gradient. (c) Individual RF traces plotted along lines representing ray paths of individual phase arrivals. (d) The corresponding common conversion point stacked image across transect; color conventions are as in panels (b) and (c), with amplitudes indicated by color bar at right (expressed as fractions of the main *P*-wave amplitude). (e) The depths of the Moho (red dots) and inferred midcrustal shear zone (blue dots) beneath each station. The color version of this figure is available only in the electronic edition.

Summary

The MAGIC geophysical experiment, which consisted of collocated linear arrays of broadband seismic and long-period MT instrumentation, was deployed in the central Appalachians between 2013 and 2016. The major scientific goals of the project are (1) to characterize the detailed seismic and electrical conductivity structure of the crust and mantle lithosphere across the central Appalachians, and to interrogate links among the geophysical structure, geological units at the surface, and neotectonic features such as the CVSZ; (2) to understand how tectonic processes associated with two complete Wilson cycles of supercontinent formation and breakup have affected the structures of the crust and lithospheric mantle; (3) to understand the processes that have modified the passive margin since the breakup of Pangea, including the lithospheric loss event that likely triggered Eocene volcanism; and (4) to understand whether and how the structure and dynamics of the lithosphere and asthenospheric mantle have contributed to the evolution of Appalachian topography through time.

Data from the MAGIC seismic and MT deployment have been used to construct images of the crust and mantle lithosphere (both seismic and electrical properties) that have begun to address this set of science questions. Specifically, we have found evidence for a midcrustal feature beneath the western portion of the MAGIC array that likely corresponds to a shear zone at the leading edge of the Grenville deformation front. Through a combination of constraints from inversion of MT data, *Sp* RF analysis, and measurements of body-wave attenuation, we have demonstrated that the lithosphere beneath the Central Appalachian Mountains is thin, suggesting a lithospheric loss event that likely took place during the Eocene, contemporaneously with anomalous intraplate volcanism. The anisotropic structure of the upper mantle beneath the central Appalachians is complex and suggests contributions from both the asthenosphere and the lithosphere, with the latter containing information about the deformation patterns that accompanied orogenesis and rifting in the past. Analysis of the MAGIC geophysical data set continues, and we are in the process of synthesizing constraints from MAGIC geophysical imaging with constraints from other investigations to gain a holistic picture of the structure, dynamics, and evolution of the central portion of the eastern North American passive margin. Data from the MAGIC experiment are publicly available via the IRIS DMC, and we strongly encourage other researchers to make use of data. The MAGIC geophysical data set demonstrates the power of carrying out collocated seismic and MT deployments, and of the joint analysis of different data sets to constrain the structure, dynamics, and evolution of the crust and upper mantle.

Data and Resources

Data from the Mid-Atlantic Geophysical Integrative Collaboration (MAGIC) experiment are publicly available via the Incorporated Research Institutions for Seismology (IRIS) Data Management Center (DMC; https://ds.iris.edu/ds/nodes/dmc). These include waveform data from the seismic experiment (network code 7A; doi: 10.7914/SN/7A_2013) and transfer functions from the magnetotelluric (MT) experiment (network code EM; doi: http://dx.doi.org/10.17611/DP/EMTF/MAGIC). Some analyses presented in this article also used data from other networks, including the U.S. National Seismic Network (network code US; doi: 10.7914/SN/US), the seismic USArray Transportable Array (network code TA; doi: 10.7914/SN/TA), the seismic central and eastern United States Network (network code N4; doi: 10.7914/SN/N4), and the MT USArray Transportable array (network code EM; doi: 10.7914/SN/EM). Data from these networks are archived by the IRIS DMC. We also used data from INTERMAGNET magnetic observatories (https://intermagnet.org). All websites were last accessed in May 2020.

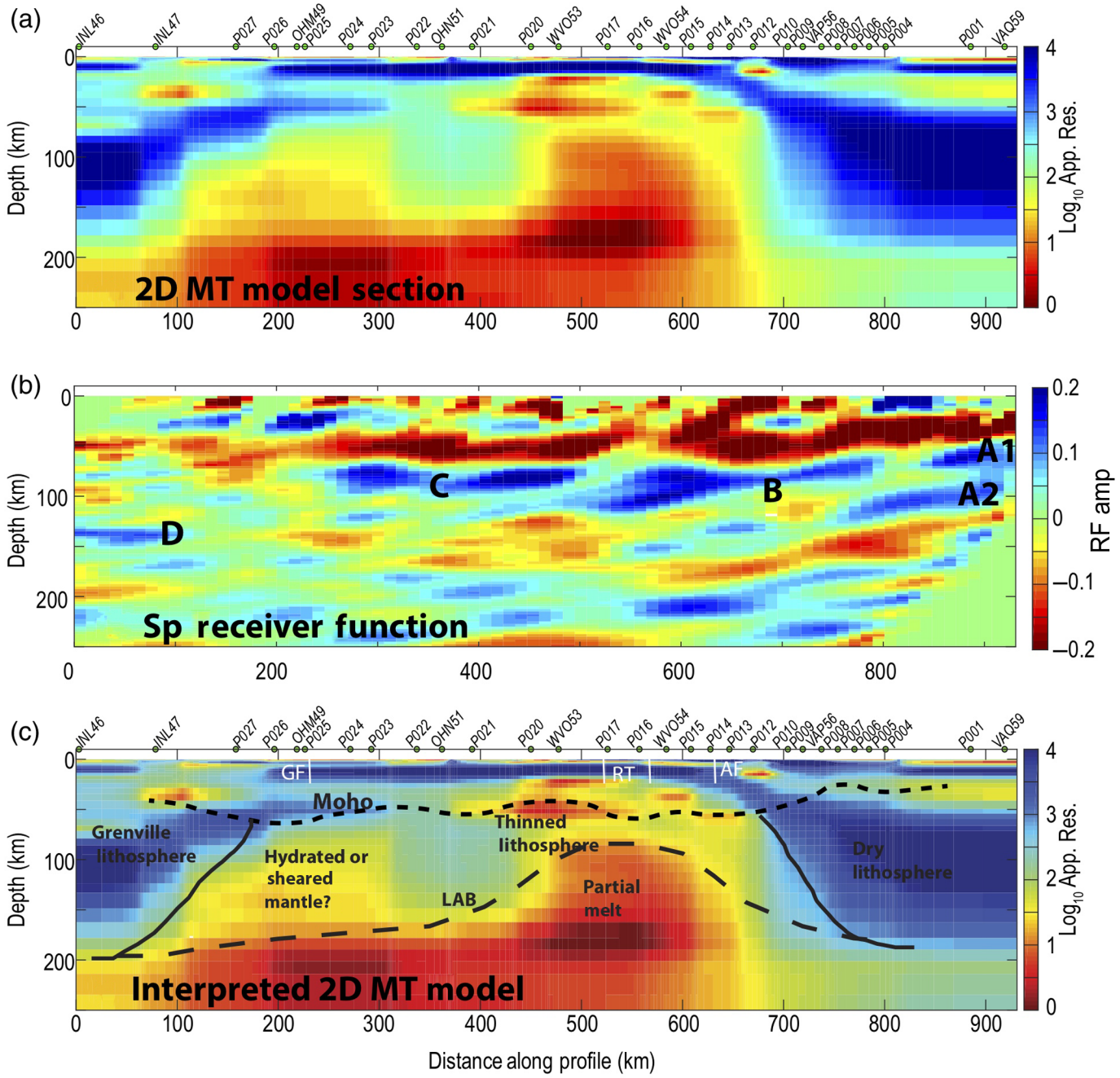

Figure 10. View of lithospheric structure across the MAGIC array provided by the electrical conductivity model and *Sp* RF analysis, modified from Evans *et al.* (2019). (a) The preferred 2D electrical conductivity model derived from MAGIC MT data, as discussed in Evans *et al.* (2019). Colors indicate resistivity values as indicated by color bar at right, with red colors indicating low resistivity and blue colors indicating high resistivity. Locations of MT stations are shown with dots at top. (b) An image of lithospheric structure derived from common conversion point stacking of *Sp* RFs. Red features indicate a positive velocity gradient with depth; blue features indicate a negative velocity gradient. Amplitudes of conversions are indicated by the color bar at right (expressed as fractions of the main *S*-wave amplitude). Major features are indicated by letters, as discussed in more detail in Evans *et al.* (2019). A1 and A2 indicate possible conversions associated with the base of the lithosphere in the eastern portion of the array. B is a shallow, westward-dipping converter that we interpret as corresponding to the base of the lithosphere beneath the Appalachian Mountains. C is a flat-lying converter that we interpret as a midlithospheric discontinuity. D is a flat-lying converter that we hypothesize corresponds to the base of the lithosphere. (c) An interpreted view of the electrical conductivity model; the interpretation is based on the models shown in panels (a) and (b). The color version of this figure is available only in the electronic edition.

Acknowledgments

The Mid-Atlantic Geophysical Integrative Collaboration (MAGIC) experiment was supported by the EarthScope and GeoPRISMS programs of the National Science Foundation (NSF) via Grant EAR-1251515 to Yale University, Grant EAR-1251329 to the College of New Jersey, and Grant EAR-1460257 to the Woods Hole Oceanographic Institution. The NSF Independent Research and Development (IRD) program helped support preparation of this article. Any opinion, findings, and conclusions or recommendations expressed in this article are those of the author and do not necessarily reflect the views of the NSF. The authors are grateful to the many landowners who hosted seismic stations during the experiment. The authors thank colleagues at colleges and universities in the MAGIC field area who provided assistance, particularly Leonard Smock and John Devincenzi (VCU), Dennis Kanach (Randolph-Macon), Liz Johnson and the late Justin Brown (JMU), Erik Klemetti (Denison), the late Ray Rataiczak (Muskingum), and Terry Sheridan (ONU). The Department of Geology and Environmental Science at JMU graciously provided space for a huddle test of instruments before deployment. The authors thank the large number of field volunteers who worked tirelessly on various phases of the MAGIC seismic deployment, many of whom were students at the College of New Jersey, Yale University, or Virginia Tech. Support from the Incorporated Research Institutions for Seismology (IRIS) Program for Array Seismic Studies of the Continental Lithosphere (PASSCAL) Instrument Center was invaluable to the success of the MAGIC seismic experiment; the authors are particularly grateful to Katyliz Anderson, Pnina Miller, Alissa Scire, and Noel Barstow. The facilities of the IRIS Consortium are supported by the National Science Foundation (NSF)'s Seismological Facilities for the Advancement of Geoscience (SAGE) Award under Cooperative Support Agreement EAR-1851048. The authors would like to thank the many landowners who gave permission for us to install magnetotelluric (MT) stations on their land. Richard Sullivan, Charlotte Wiman, Eric Attias, Shane McGary, Reagan Cronin, Marah Dahn, Andy Frassetto, and Kyle Jones are thanked for their help in the field with the MT deployment. Xavi Garcia provided his expertise and code in processing some of the more problematic MT stations. This article used data from INTERMAGNET magnetic observatories. The authors thank the national institutes that support them and INTERMAGNET for promoting high standards of magnetic observatory practice. The authors are grateful to Paul Wiita and David McGee at the College of New Jersey for their help facilitating aspects of this work, and to our scientific collaborators on the MAGIC project, particularly co-PIs Scott King (Virginia Tech) and Eric Kirby (Oregon State). The authors thank our coauthors and collaborators on various articles and projects that use data from the experiment. Figures were generated using the Generic Mapping Tools (Wessel and Smith, 1999), the Seismic Analysis Code (SAC; Goldstein *et al.*, 2003), and the IRIS DMC data quality analysis tools (e.g., Casey *et al.*, 2018). Finally, the authors thank the associate editor, an anonymous reviewer, and Benjamin Murphy for thoughtful comments that helped us improve the article.

References

Aragon, J. C., M. D. Long, and M. H. Benoit (2017). Lateral variations in *SKS* splitting across the MAGIC array, central Appalachians, *Geochem. Geophys. Geosyst.* **18,** 4136–4155, doi: 10.1002/2017GC007169.

Biryol, C. B., L. S. Wagner, K. M. Fisher, and R. B. Hawman (2016). Relationship between observed upper mantle structures and recent tectonic activity across the southeastern United States, *J. Geophys. Res.* **121,** 3393–3414, doi: 10.1002/2015JB012698.

Borden, S., P. Mondal, and M. D. Long (2019). Probabilistic finite frequency SKS splitting intensity tomography: Applications to South America and the Central Appalachians, *AGU Fall Meeting*, San Francisco, California, Abstract S41D-0560.

Byrnes, J. S., M. Bezada, M. D. Long, and M. H. Benoit (2019). Thin lithosphere beneath the central Appalachian Mountains: Constraints from seismic attenuation beneath the MAGIC array, *Earth Planet. Sci. Lett.* **519,** 297–307, doi: 10.1016/j.epsl.2019.04.045.

Caldwell, T. G., H. M. Bibby, and C. Brown (2004). The magnetotelluric phase tensor. *Geophys. J. Int.* **158,** 457–469, doi: 10.1111/j.1365-246X.2004.02281.x.

Casey, R., M. E. Templeton, G. Sharer, L. Keyson, B. Weertman, and T. Ahern (2018). Assuring the quality of IRIS data with MUSTANG, *Seismol. Res. Lett.* **89,** 630–639, doi: 10.1785/0220170191.

Chave, A. D., and D. J. Thomson (2004). Bounded influence magnetotelluric response function estimation, *Geophys. J. Int.* **157,** 988–1006, doi: 10.1111/j.1365-246X.2004.02203.x.

Elling, R. P., S. Stein, C. A. Stein, and G. R. Keller (2020). Tectonic implications of the gravity signatures of the Midcontinent Rift and Grenville Front, *Tectonophysics* **778,** 228,369, doi: 10.1016/j.tecto.2020.228369.

Evans, R. R., M. H. Benoit, M. D. Long, J. Elsenbeck, H. A. Ford, J. Zhu, and X. Garcia (2019). Thin lithosphere beneath the central Appalachian Mountains: A combined seismic and magnetotelluric study, *Earth Planet. Sci. Lett.* **519,** 308–316, doi: 10.1016/j.epsl.2019.04.46.

Ferguson, I. J. (2012). Instrumentation and field procedures, in *The Magnetotelluric Method: Theory and Practice*, A. D. Chave and A. G. Jones (Editors), Chapter 9, Cambridge University Press, 421–479, doi: 10.1017/CBO9781139020138.011.

Fischer, K. M. (2002). Waning buoyancy in the crustal roots of old mountains, *Nature* **417,** 933–936, doi: 10.1038/nature00855.

Frizon de Lamotte, D., B. Fourdan, S. Leleu, F. Leparmentier, and P. de Clarens (2015). Style of rifting and the stages of Pangea breakup, *Tectonics* **34,** 1009–1029, doi: 10.1002/2014TC003760.

Goldstein, P., D. Dodge, M. Firpo, and L. Minner (2003). SAC2000: Signal processing and analysis tools for seismologists and engineers, in *The IASPEI International Handbook of Earthquake and Engineering Seismology*, W. H. K. Lee, H. Kanamori, P. C. Jennings, and C. Kisslinger (Editors), Academic Press, London.

Hatcher, R. D., Jr. (2010). The Appalachian orogeny: A brief summary, in *From Rodinia to Pangea: The Lithotectonic Record of the Appalachian Region*, R. P. Tollo, M. J. Bartholomew, J. P. Hibbard, and P. M. Karabinos (Editors), Geol. Soc. Am. Memoir 206, 1–19, doi: 10.1130/2010.1206(01).

Hibbard, J. P., C. R. van Staal, and D. W. Rankin (2010). Comparative analysis of the geological evolution of the northern and southern Appalachian orogeny, in *From Rodinia to Pangea: The Lithotectonic Record of the Appalachian Region*, R. P. Tollo, M. J. Bartholomew, J. P. Hibbard, and P. M. Karabinos (Editors), Geol. Soc. Am. Memoir 206, 51–69, doi: 10.1130/2010.1206(03).

Hopper, E., K. M. Fischer, L. S. Wagner, and R. B. Hawman (2017). Reconstructing the end of the Appalachian orogeny, *Geology* **45,** 15–18, doi: 10.1130/G38453.1.

Kintner, J. A., C. J. Ammon, K. Homman, and A. Nyblade (2020). Precise relative magnitude and relative location estimates of low-yield industrial blasts in Pennsylvania, *Bull. Seismol. Soc. Am.* **110,** 226–240, doi: 10.1785/012019163.

Lai, H., E. J. Garnero, S. P. Grand, R. W. Porritt, and T. W. Becker (2019). Global travel time data set from adaptive empirical wavelet construction, *Geochem. Geophys. Geosyst.* **20,** 2175–2198, doi: 10.1029/2018GC007905.

Li, L., T. Lay, K. F. Cheung, and L. Ye (2016). Joint modeling of teleseismic and tsunami wave observations to constrain the 16 September 2015 Illapel, Chile, M_w 8.3 earthquake rupture processes, *Geophys. Res. Lett.* **43,** 4304–4312, doi: 10.1002/2016GL068674.

Li, X. Z., S. V. Bogdanova, A. S. Collins, A. Davidson, B. De Waele, R. E. Ernst, I. C. W. Fitzsimons, R. A. Fuck, D. P. Gladkochub, J. Jacobs, *et al.* (2008). Assembly, configuration, and break-up history of Rodinia: A synthesis, *Precamb. Res.* **160,** 179–210, doi: 10.1016/j.precamres.2007.04.021.

Liu, S., and S. D. King (2019). A benchmark study of incompressible Stokes flow in a 3-D spherical shell using ASPECT, *Geophys. J. Int.* **217,** 650–667, doi: 10.1093/gji/ggz036.

Liu, S., J. C. Aragon, M. H. Benoit, M. D. Long, and S. D. King (2018). Transition zone structure beneath the eastern U.S., *AGU Fall Meeting*, Washington, D.C., Abstract T52D-05.

Long, M. D., and M. H. Benoit (2017). Structure of the crust and mantle lithosphere beneath the central Appalachians: Results from the MAGIC experiment (Paper number 29-8), *Geol. Soc. Am. Abstr. Prog.* **49,** no. 6, doi: 10.1130/abs/2017AM-304038.

Long, M. D., M. H. Benoit, J. C. Aragon, and S. D. King (2019). Seismic imaging of mid-crustal structure beneath central and eastern North America: Possibly the elusive Grenville deformation? *Geology* **47,** 371–374, doi: 10.1130/G46077.1.

Lynner, C., and M. Bodmer (2017). Mantle flow along the eastern North American margin inferred from shear wave splitting, *Geology* **47,** 867–807, doi: 10.1130/G38980.1.

Lynner, C., H. J. A. Van Avendonk, A. Bécel, G. L. Christeson, B. Dugan, J. B. Gaherty, S. Harder, M. J. Hornbach, D. Lizzarralde, M. D. Long, *et al.* (2020). The eastern North American margin community seismic experiment: An amphibious active- and passive-source dataset, *Seismol. Res. Lett.* **91,** 533–540, doi: 10.1785/0220190142.

Mazza, S. E., E. Gazel, E. A. Johnson, M. Bizimis, R. McAleer, and C. B. Biryol (2017). Post-rift magmatif evolution of the eastern North American "passive-aggressive" margin, *Geochem. Geophys. Geosyst.* **18,** 3–22, doi: 10.1002/2016GC006646.

Mazza, S. E., E. Gazel, E. A. Johnson, M. J. Kunk, R. McAleer, J. A. Spotila, M. Bizimis, and D. S. Coleman (2014). Volcanoes of the passive margin: The youngest magmatic event in eastern North America, *Geology* **42,** 483–486, doi: 10.1130/G35407.1.

McLelland, J. M., M. W. Selleck, and M. E. Bickford (2010). Review of the Proterozoic evolution of the Grenville Province, its Adirondack outlier, and the Mesoproterozoic inliers of the Appalachians, in From *Rodinia to Pangea: The Lithotectonic Record of the Appalachian Region*, R. P. Tollo, M. J. Bartholomew, J. P. Hibbard, and P. M. Karabinos (Editors), Geol. Soc. Am. Memoir 206, 21–49, doi: 10.1130/2010.1206(02).

McNamara, D. E., H. M. Benz, R. B. Herrmann, E. A. Bergman, P. Earle, A. Meltzer, M. Withers, and M. Chapman (2014). The M_w 5.8 Mineral, Virginia, earthquake of August 2011 and aftershock sequence: Constraints on earthquake source parameters and fault geometry, *Bull. Seismol. Soc. Am.* **104,** 40–54, doi: 10.1785/0120130058.

Miller, S. R., E. Kirby, M. D. Long, M. H. Benoit, S. D. King, P. R. Bierman, and P. B. Sak (2015). Late Cenozoic topographic rejuvenation in the central Appalachians: Geomorphic constraints and geophysical relationships from the MAGIC project, *GSA Annual Meeting*, Baltimore, Maryland, Abstract 268-5.

Miller, S. R., P. B. Sak, E. Kirby, and P. R. Bierman (2013). Neogene rejuvenation of central Appalachian topography: Evidence for differential rock uplift from stream profiles and erosion rates, *Earth Planet. Sci. Lett.* **369,** 1–12, doi: 10.1016/j.epsl.2013.04.007.

Mondal, P., and M. D. Long (2019). A model space search approach to finite-frequency SKS splitting intensity tomography in a reduced parameter space, *Geophys. J. Int.* **217,** 238–256, doi: 10.1093/gji/ggz016.

Moucha, R., A. M. Forte, J. X. Mitrovica, D. B. Rowley, S. Quéré, N. A. Simmons, and S. P. Grand (2008). Dynamic topography and long-term sea-level variations: There is no such thing as a stable continental platform, *Earth Planet. Sci. Lett.* **271,** 101–108, doi: 10.1016/j.epsl.2008.03.056.

Neukirch, M., and X. Garcia (2014). Nonstationary magnetotelluric data processing with instantaneous parameter, *J. Geophys. Res.* **119,** 1634–1654, doi: 10.1002/2013JB010494.

Peterson, J. (1993). Observations and modeling of seismic background noise, *U.S. Geol. Surv. Open-File Rept.* 93-322, doi: 10.3133/ofr93322.

Rivers, T. (1997). Lithotectonic elements of the Grenville Province: Review and tectonic implications, *Precamb. Res.* **86,** 117–154, doi: 10.1016/S0301-9268(97)0038-7.

Schulte-Pelkum, V., G. Monsalve, A. Sheehan, M. R. Pandey, S. Sapkota, R. Bilham, and F. Wu (2005). Imaging the Indian subcontinent beneath the Himalaya, *Nature* **435,** 1222–1225, doi: 10.1038/nature03678.

Servali, A., M. D. Long, J. Park, M. H. Benoit, and J. C. Aragon (2020). Love-to-Rayleigh scattering across the eastern North American passive margin, *Tectonophysics* **776,** 228,321, doi: 10.1016/j.tecto.2020.228321.

Spasojevic, S., L. Liu, M. Gurnis, and R. D. Müller (2008). The case for dynamic subsidence of the U.S. east coast since the Eocene, *Geophys. Res. Lett.* **35,** L08305, doi: 10.1029/2008GL033511.

Stein, C. A., S. Stein, R. Elling, G. R. Keller, and J. Kley (2018). Is the "Grenville Front" in the central United States really the Midcontinent Rift? *GSA Today* **28,** 4–10, doi: 10.1130/GSATG357A.1.

Steltenpohl, M. G., I. Zietz, J. W. Horton Jr., and D. L. Daniels (2010). New York-Alabama lineament: A buried right-slip fault bordering the Appalachians and mid-continent North America, *Geology* **38,** 571–574, doi: 10.1130/G30978.1.

Tape, C., D. C. Heath, M. G. Baker, S. Dalton, K. Aderhold, and M. E. West (2019). Bear encounters with seismic stations in Alaska and Northwestern Canada, *Seismol. Res. Lett.* **90,** 1950–1970, doi: 10.1785/0220190081.

Wagner, L. S., K. M. Fischer, R. Hawman, E. Hopper, and D. Howell (2018). The relative roles of inheritance and long-term passive margin lithospheric evolution on the modern structure and tectonic activity in the southeastern United States, *Geosphere* **14,** 1385–1410, doi: 10.1130/GES01593.1.

Wessel, P., and W. H. F. Smith (1999). Free software helps map and display data, *Eos Trans. AGU* **72,** 441–446, doi: 10.1029/90EO00319.

Whitmeyer, S., and K. Karlstrom (2007). Tectonic model for the Proterozoic growth of North America, *Geosphere* **3,** 220–259, doi: 10.1130/GES00055.1.

Wolin, E., S. Stein, F. Pazzaglia, A. Meltzer, A. Kafka, and C. Berti (2012). Mineral, Virginia, earthquake illustrates seismicity of a passive-aggressive margin, *Geophys. Res. Lett.* **39,** L02305, doi: 10.1029/2011GL050310.

Manuscript received 27 April 2020
Published online 1 July 2020